Article

Current Biology

Floral Pigmentation Has Responded Rapidly to Global Change in Ozone and Temperature

Highlights

- Globally, UV-absorbing pigmentation of flowers increased during the 20th century
- Pigmentation increased with ozone decline in taxa with pollen exposed to ambient UV
- Pigmentation declined with temperature rise in taxa with pollen shielded by petals
- Rapid floral pigmentation responses to global change may impact pollination

Authors

Matthew H. Koski, Drew MacQueen, Tia-Lynn Ashman

Correspondence

mkoski@clemson.edu

In Brief

Koski et al. show that ozone declines contributed to increases in UV-absorbing floral pigmentation while climate warming contributed to pigmentation declines in some taxa. Across taxa, the severity of climatic change predicted the amount of pigmentation change. Flower color responses to a global change could impact plant-pollinator interactions.

Koski et al., 2020, Current Biology *30*, 1–7
November 16, 2020
https://doi.org/10.1016/j.cub.2020.08.077

CellPress

Please cite this article in press as: Koski et al., Floral Pigmentation Has Responded Rapidly to Global Change in Ozone and Temperature, Current Biology (2020), https://doi.org/10.1016/j.cub.2020.08.077

Current Biology

CellPress
OPEN ACCESS

Article

Floral Pigmentation Has Responded Rapidly to Global Change in Ozone and Temperature

Matthew H. Koski,[1,2,5,6,*] Drew MacQueen,[3] and Tia-Lynn Ashman[4]
[1]Clemson University, Department of Biological Sciences, Clemson, SC 29631, USA
[2]University of Virginia, Department of Biology, Charlottesville, VA 22904, USA
[3]University of Virginia Library Scholars Lab, PO Box 40010, Charlottesville, VA 22904-4129, USA
[4]University of Pittsburgh, Department of Biological Sciences, Pittsburgh, PA 15260, USA
[5]Twitter: @mhkoski
[6]Lead Contact
*Correspondence: mkoski@clemson.edu
https://doi.org/10.1016/j.cub.2020.08.077

SUMMARY

Across kingdoms, organisms ameliorate UV stress by increasing UV-absorbing pigmentation. Rapid ozone degradation during the 20th century resulted in elevated UV incidence, but pigmentation responses to this aspect of global change have yet to be demonstrated. In flowering plants, UV exposure favors larger areas of UV-absorbing pigmentation on petals, which protects pollen from UV-damage. Pigmentation also affects floral thermoregulation, suggesting climate warming may additionally impact pigmentation. We used 1,238 herbarium specimens collected from 1941 to 2017 to test whether change in UV floral pigmentation was associated with altered ozone and temperature in 42 species spanning three continents. We tested three predictions: first, UV-absorbing pigmentation will increase temporally and be correlated with reduced ozone (higher UV) when accounting for effects of temperature; second, taxa that experienced larger ozone declines will display larger increases in pigmentation; and third, taxa with anthers exposed to ambient UV will respond more strongly than those with anthers protected by petals. Globally, the extent of petal UV pigmentation increased significantly across taxa by ~2% per year. However, temporal change was species specific—increasing in some taxa but declining in others. Species with exposed anthers experiencing larger declines in ozone displayed more dramatic pigmentation increases. For taxa with anthers enclosed within petals, pigmentation declined with increases in temperature, supporting a thermoregulatory role of UV pigmentation. Results document a rapid phenotypic response of floral pigmentation to anthropogenic climatic change, suggesting that global change may alter pollination through its impact on floral color, with repercussions for plant reproductive fitness.

INTRODUCTION

Anthropogenic disruption of tropospheric ozone resulted in rapid increases of ultraviolet (UV) irradiance reaching Earth's terrestrial and aquatic systems (e.g., as much as a 35% increase from 1979–2008 [1]), and in some regions, this trend will continue despite successful efforts to curb ozone degradation (e.g., [2–4]). UV-B exposure negatively impacts many aspects of organismal health (reviewed in [5]), so elevated UV could drive coordinated phenotypic responses in traits that ameliorate UV stress such as pigmentation, much like altered temperature and precipitation regimes have elicited ecological and evolutionary responses [6–10]. Documenting phenotypic responses to rapid increases in UV exposure is crucial for holistically understanding the legacy of recent anthropogenic global change as well as predicting evolutionary trajectories under ongoing climatic change.

Darker pigmentation is under particularly strong selection by UV-B irradiance [5]. The primary mode of UV damage to DNA is the formation of pyrimidine-dimers, which, if left unrepaired, inhibit DNA replication [11]. UV-absorbing pigmentation serves as a UV-protecting mechanism in humans [12], bacteria [13], crustaceans [14], insects [15], non-human primates [16], and plants [17, 18], providing a striking cross-kingdom example of convergence. In plants, the accumulation of UV-absorbing pigments (e.g., flavonoids) in epidermal tissue is a primary mechanism of UV photoprotection [19] and UV-absorbing compounds are generally increased in response to ozone depletion [20]. One study revealed that UV-absorbing flavonoid concentration of an Antarctic moss increased in response to declining ozone and increasing UV [21]; but whether ozone decline has driven changes in pigmentation across a wide diversity of taxa and whether species' responses depend on the magnitude of ozone depletion has yet to be revealed.

Many flowering plants have spatially variable UV absorption/reflection on their petals forming a UV "bullseye" (Figure 1B). Flavonoids, a group of secondary plant metabolites, are often responsible for floral UV absorption [22–26]. The proportional area of petals that absorbs UV (UV proportion [UVP]) is heritable [27–29] and, in one taxon, did not display plasticity in response to

Please cite this article in press as: Koski et al., Floral Pigmentation Has Responded Rapidly to Global Change in Ozone and Temperature, Current Biology (2020), https://doi.org/10.1016/j.cub.2020.08.077

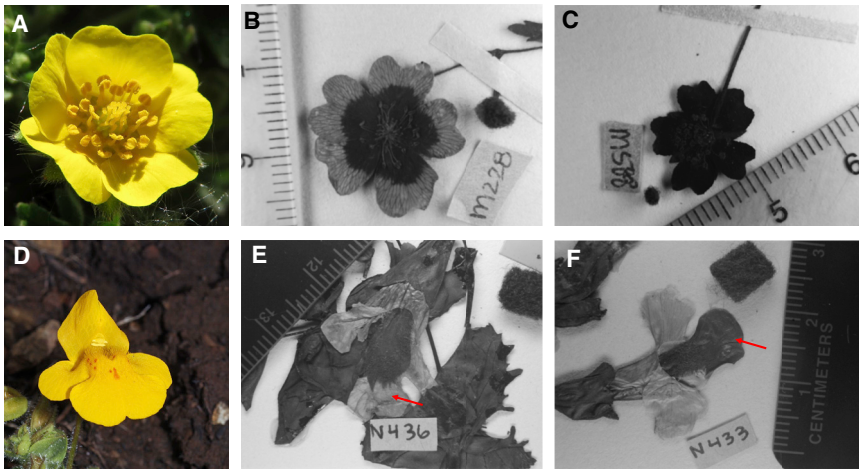

Figure 1. Examples of Variation in Ultraviolet (UV) Floral Pigmentation

Exemplary images for a species with anthers exposed to ambient conditions, *Potentilla crantzii* (A–C) and a species with anthers protected by floral tissue *Mimulus guttatus* (D–F). Darker petal areas possess UV-absorbing compounds whereas lighter areas are UV reflective and lack UV-absorbing compounds. (B) and (E) display a reduced area of UV-absorbing pigmentation on petals compared to (C) and (F). Arrows in (E) and (F) highlight differences in pigment distribution on the lower petal lobe of *M. guttatus*.

UV light exposure [30]. While the UV bullseye phenotype serves as a visual cue for UV-perceptive pollinators [31–34], floral UV absorption also ameliorates UV damage to pollen grains, which house the male gametes in flowering plants [17]. A larger area of UV absorption attenuates UV, reducing the reflection of UV light from petals onto pollen-producing anthers. Experiments show that flowers with larger proportional areas of UV absorption on petals have elevated pollen viability under UV stress [17]. Geographic regions that experience higher UV-B (e.g., lower latitude and high altitude) are populated by plants with larger UVP, which has been supported both within a widely distributed herb *Argentina anserina* as well as among nearly 200 related species [17, 35].

Because UV irradiance drives spatial patterns in UV floral pigmentation [17, 35], it stands to reason that temporal declines in ozone and concomitant increases in UV may have driven increases of UV-absorbing floral pigmentation. Phenotypic responses, however, may depend on factors such as floral morphology, life history, or the local magnitude of change in ozone or other climatological factors experienced by a given species. For example, pigmentation responses to elevated UV may be minimal for flowers whose anthers are not exposed to ambient photic conditions because petals protect pollen-filled anthers from exposure by absorbing or reflecting UV. In contrast, more pronounced responses are predicted for flowers with anthers exposed to ambient UV light, where UV radiation should be a stronger agent of selection on pigmentation [36]. Additionally, plants with shorter generation times may have increased adaptive potential due to reduced time to reproduction and increased establishment of novel genotypes compared to perennial plants [37, 38]. Finally, rising temperatures may also elicit phenotypic responses in floral pigmentation [39]. Darker flowers are often favored in cooler environments because elevated light absorption can warm reproductive structures (see [40] and references therein). Thus, incorporating an understanding of how temperature covaries with pigmentation is crucial for isolating the direct effects of changing ozone.

Museum specimens provide an unparalleled retrospective view of phenotypes, species interactions, and phenologies [41, 42]. Tracking pigmentation change in plants, however, can be difficult because visible floral pigments (e.g., anthocyanins, carotenoids) often degrade rapidly in dried herbarium specimens. An exception is UV-absorbing flavonoids, which are retained in dried plant specimens. Floral UV patterning is measurable on herbarium records using UV photography, providing a "time capsule" of historical phenotypes [35, 43] (Figure 1). We measured UV pigmentation of 1,238 flowers on herbarium specimens spanning a 77-year period for 42 species (18 families; 22 genera) across three continents (Figure S1; Table S1). We assessed how pigmentation covaries with historical ozone and temperature. With this dataset we test the following predictions: (1) the size of the UV-absorbing area on flowers will increase over time, (2) if UV is a driver of variation in pigmentation, there will be a negative relationship between ozone and pigmentation when accounting for the effects of temperature, and (3) species that experienced more dramatic temporal declines in ozone will display larger increases in pigmentation than those experiencing lower declines in ozone. We assessed species with exposed anthers (radially symmetric, actinomorphic) and concealed anthers (bilaterally symmetric, zygomorphic) to test the prediction that those with exposed anthers will display a more pronounced response to ozone declines than those with concealed anthers.

RESULTS

Floral Pigmentation Increased over 76 Years but Temporal Change Varied across Taxa

Across all taxa, the UVP increased annually by an estimated 2% (+/− 0.5% SE) on average when accounting for taxonomic, geospatial, and seasonal effects on pigmentation (Table 1; year effect, $p = 0.018$; year parameter estimate = 0.0198, +/−0.00498 SE, $t = 3.98$, $p < 0.0001$). Despite an average increase in pigmentation across all species, temporal change was highly taxon specific (Table 1A; species × year effect, $p < 0.001$) with some taxa decreasing in pigmentation or showing no change (Figure 2). Contrary to predictions, positive effect sizes of year on petal pigmentation were not restricted to flowers with anthers exposed to ambient light conditions. The effect size of year on UVP was positive in both taxa with anthers concealed within petal tissue (50%, 6 of 12) and those with exposed anthers (43%, 15 of 33) (Figure 2). The effect size of year on UVP for taxa that increased in pigmentation was on average 70% higher

Please cite this article in press as: Koski et al., Floral Pigmentation Has Responded Rapidly to Global Change in Ozone and Temperature, Current Biology (2020), https://doi.org/10.1016/j.cub.2020.08.077

CellPress
OPEN ACCESS

Table 1. Spatiotemporal Effects on Ultraviolet Floral Pigmentation

Source	DF	F Value	*P*
Species nested in shape	39	1.87	0.001
Floral shape	1	4.95	0.026
Latitude (absolute)	1	10.23	0.001
Longitude	1	10.71	0.001
Altitude	1	2.84	0.092
Year	1	5.66	0.018
Month nested in continent	32	3.81	<.0001
Shape × latitude	1	7.98	0.005
Shape × longitude	1	6.54	0.011
Shape × altitude	1	0.79	0.373
Shape × month	20	7.39	<.0001
Shape × year	1	1.46	0.227
Species × year	43	2.19	<.0001

Results from a mixed linear model testing for temporal change in pigmentation across 42 species while accounting for species identity, floral shape (anthers exposed versus concealed), geospatial effects (latitude, longitude, altitude), and seasonal effects (month). Continent (Australia, Eurasia, North America) was a random effect in the model. Pigmentation was measured as the proportion of petal area that absorbs UV (UV proportion; UVP). Model results are from analyses using Type III sums of squares.

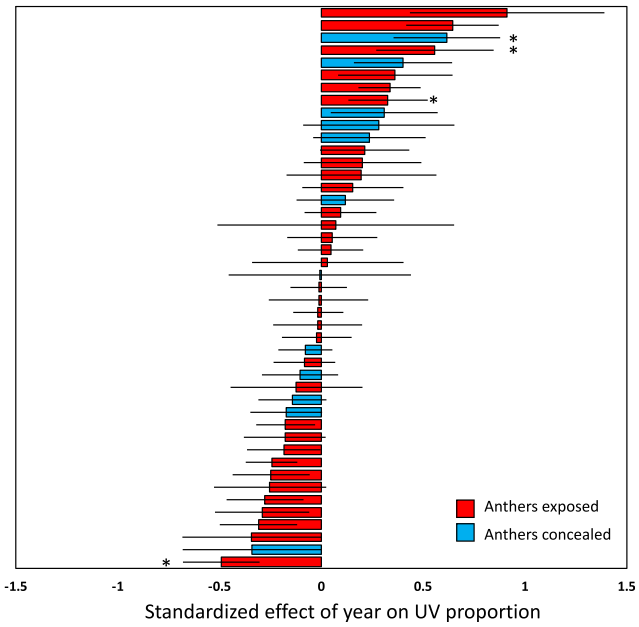

Figure 2. Temporal Change in Floral UV Pigmentation Was Positive on Average for 45 Taxa, but Taxa Varied in the Direction and Magnitude of Temporal Phenotypic Change

The plot shows standardized slopes of UV proportion on the year of specimen collection for each taxon, with SEs calculated from general linear models accounting for geospatial and seasonal effects. UV proportion is calculated as the relative area of a petal that absorbs UV. (Table 1; year and species × year effects). Asterisks indicate a significant effect of year on pigmentation for a given species.

than the magnitude of the effect size of year for taxa that decreased in pigmentation (Figure 2), driving the overall positive effect of year on pigmentation.

Reduced Ozone Is Directly Linked with Elevated Pigmentation in Species with Exposed Anthers

We tested whether UV floral pigmentation was directly linked to historic monthly average stratospheric ozone level at the time of collection for each specimen while accounting for species identity and temperature using a general linear model. The model revealed that ozone had a negative effect on pigmentation in taxa with exposed anthers—UVP was higher under lower ozone levels (higher UV) (Figure 3; Table 2; floral shape × ozone effect, $p < 0.001$). However, ozone had the opposite effect on UV pigmentation in species with concealed anthers (Figure 3; Table 2; floral shape × ozone effect, $p < 0.001$). Thus, ozone decline is implicated as a factor contributing to increased pigmentation only in taxa whose flowers have exposed anthers.

Magnitude of Climatic Change and Floral Shape Predict Phenotypic Change

Because we detected pronounced species-specific change in floral pigmentation across time (Figure 2; Table 1), we tested whether differential responses among taxa were due to variation in the magnitude of climatic change experienced and/or species attributes. For each species, we calculated the effect of size of the year on UVP, ozone, and temperature. We then modeled the change in UVP over time as a function of the change in ozone and temperature over time, floral shape, life history (long-lived versus short-lived), and habitat affinity (shaded versus open). There was a significant negative effect of ozone change on pigmentation change for species with exposed anthers but not for species with concealed anthers (Figure 4A; Table 3). Specifically, species with concealed anthers that experienced larger ozone declines over time displayed larger increases in pigmentation (UVP change = −0.44(ozone change) − 0.018, $R^2 = 0.16$, $F_{1,31} = 5.87$, $p = 0.02$; Figure 4A). Pigmentation change in species with concealed anthers, however, was unrelated to ozone change (UVP change = −0.15(ozone change) + 0.10, $R^2 = 0.02$, $F_{1,10} = 0.26$, $p = 0.62$; Figure 4A).

Temperature change also had an effect on UV pigmentation change, but the effect depended on whether a flower had concealed or exposed anthers (Figure 4B; Table 3). Species with concealed anthers that experienced increases in temperature over time decreased in floral pigmentation (UVP = −0.66(temp) + 0.14, $R^2 = 0.42$, $F_{1,10} = 7.3$, $p = 0.02$; Figure 4B), while those with exposed anthers displayed the opposite pattern (UVP = 0.45(temp) − 0.004, $R^2 = 0.13$, $F_{1,31} = 4.57$, $p = 0.04$; Figure 4B).

We used a phylogenetically informed analysis to test whether results were robust to species relatedness. This analysis again revealed strong effects of floral shape × ozone change and the shape × temperature change (Table 3). Additional effects of habitat affinity (shaded versus open) and life history (short-lived versus long-lived) were revealed with the phylogenetic generalized least squares (PGLS) model (Table 3). Specifically, the effect size of year on pigmentation was larger for species in open habitat than those in understory shaded habitat (effect size of year on UVP; open habitat = 0.067 ± 0.048 SE; shaded habitat = −0.132 ± 0.089 SE). And, the effect size of year on pigmentation was larger for long-lived species than short-lived species (year

Please cite this article in press as: Koski et al., Floral Pigmentation Has Responded Rapidly to Global Change in Ozone and Temperature, Current Biology (2020), https://doi.org/10.1016/j.cub.2020.08.077

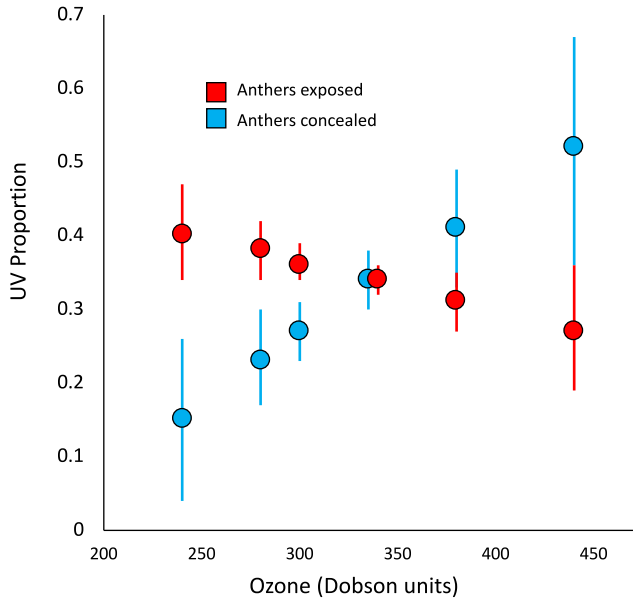

Figure 3. Reduced Ozone Is Directly Linked to Increased UV Pigmentation in Flowers with Anthers Exposed to Ambient Light Conditions

The plot displays the predicted marginal effects of ozone on UV proportion from a general linear model of UV proportion as a function of species identity, floral shape, monthly average ozone, and monthly average temperature (see Table 2). Error bars represent 95% confidence intervals for the predicted effects. There is a significant interaction between floral shape and ozone (Table 2; shape x ozone; $p < 0.0001$).

effect size on UVP; short-lived = 0.005 ± 0.10 SE; long-lived = 0.053 ± 0.049 SE).

DISCUSSION

This study documents rapid responses of floral pigmentation to anthropogenic climatic change and dissects causes of differential responses among taxa. Across a geographically and taxonomically diverse set of species, the magnitude and direction of change in UV floral pigmentation was strongly associated with the magnitude of climatic change experienced and floral morphology. This is the first study to link variability in temporal change in pigmentation among taxa to the magnitude of ozone and temperature change experienced. Notable studies in birds have shown temporal changes in melanism in single species associated with temperature increases [44–46], but here we demonstrate an association of pigmentation change with changes in ozone in addition to temperature across many species of flowering plants. Our study corroborates and extends this small set of studies showing rapid change in pigmentation in response to anthropogenic global change in plants [21].

We predicted that pigmentation would increase in response to temporal declines in ozone and concomitant increases in UV irradiance and that this response would be more pronounced in species with anthers that are exposed to ambient irradiance. However, the observed increase in pigmentation over time across all taxa was driven by pigmentation increases in both taxa with exposed and protected anthers (Figure 2). For example, *Velleia paradoxa*, a species with anthers protected within the corolla, increased significantly in floral pigmentation over time (~6% per year ± 2.6%, $p = 0.03$). However, there was only a direct negative relationship between ozone and pigmentation for taxa with anthers exposed to ambient light (Figure 3), as predicted if elevated pigmentation protects pollen from UV damage [17]. A direct negative relationship between ozone and pigmentation was not observed in taxa with concealed anthers—in fact, the relationship was reversed (Figure 3). These results suggest that the effects of UV light on floral pigmentation depend on floral shape and that pigmentation change over time in species with concealed anthers may be driven by factors other than UV exposure.

Despite the average increase in pigmentation over time, many taxa displayed little change or even declined in pigmentation (Figure 2). We were able to explain variation in temporal change in pigmentation by a combination of species attributes and the magnitude of climatic change experienced. Taxa with anthers exposed to ambient light conditions that experienced more dramatic reductions in ozone responded with elevated floral pigmentation (Figure 4). This was not the case for taxa with concealed anthers (Figure 4). Because declining ozone was only associated with elevated pigmentation in taxa with exposed anthers, the data support previous work showing that UV irradiance favors increased pigmentation through protecting pollen in open "bowl-shaped" flowers [17]. The causes of floral pigmentation change may stem from regulation of photoprotective pigments within flowers or plant-wide in response to UV exposure [18]. However, if plant-wide upregulation of UV-compounds were responsible for the increases in floral pigmentation observed, we would expect to see taxa with concealed anthers increase in pigmentation with declining ozone, which was not the case (Figure 4).

The magnitude of temperature change that a species experienced also affected pigmentation change, but the effect depended on anther exposure. For species with anthers enclosed within petal tissue, temperature increases over time resulted in reduced pigmentation whereas temperature declines resulted in increased pigmentation (Figure 4). Elevated floral pigmentation in cooler environments increases the absorption of radiative heat, more efficiently warming reproductive structures [47]. Conversely, reduced pigmentation can alleviate heat gain under high temperatures [40]. Results show that warming has resulted in decreased pigmentation for some taxa (Figure 4), indicating a

Table 2. Effect of Ozone on Ultraviolet Floral Pigmentation

Source	DF	F Value	*P*
Species nested in shape	43	14.93	<.0001
Floral shape	1	13.85	<.0001
Temperature	1	2.7	0.100
Ozone	1	2.41	0.121
Shape × ozone	1	12.65	<.0001

Results from a mixed linear model testing for the effect of ozone on floral pigmentation across 45 taxa while accounting for species identity, floral shape (anthers exposed versus concealed), and temperature. Continent (Australia, Eurasia, North America) was a random effect in the model. Model results are from analyses using Type III sums of squares.

Please cite this article in press as: Koski et al., Floral Pigmentation Has Responded Rapidly to Global Change in Ozone and Temperature, Current Biology (2020), https://doi.org/10.1016/j.cub.2020.08.077

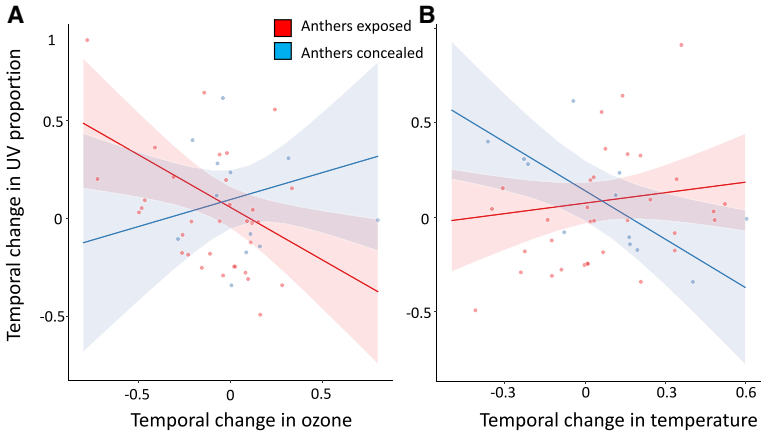

Figure 4. The Magnitude of Climatic Change Predicts Variation in the Magnitude of Temporal Change in UV Floral Pigmentation among Taxa

(A) Taxa with exposed anthers that experienced larger declines in ozone over time increased in pigmentation (b = −0.44, R^2 = 0.16, p = 0.02) whereas those with concealed anthers did not (b = 0.15, R^2 = 0.02, p = 0.62).

(B) Taxa with exposed anthers that experienced larger increases in temperature over time increased in pigmentation (b = 0.45, R^2 = 0.13, p = 0.04) whereas those with concealed anthers declined in pigmentation (b = −0.66, R^2 = 0.42, p = 0.02). Each point represents a single taxon. The x axes are the standardized effects of year of specimen collection on ozone and temperature for each species, and the y axes are standardized effects of year of collection on UV proportion. Results are robust to shared evolutionary history among species (Table 3).

potential role of UV pigmentation in floral thermoregulation. This response may be isolated to taxa with concealed anthers because high temperatures may be a stronger selective agent in these taxa compared to those with exposed reproductive structures. For example, the morphology of some species with enclosed reproductive structures creates a "microgreenhouse" effect, trapping incident light and re-radiating it within the flower [40]. High temperature stress can render pollen infertile (e.g., [48]), and it follows that heat stress should favor mechanisms to reduce floral temperatures. In taxa with exposed anthers, those experiencing increases in temperature tended to increase in pigmentation (Figure 4). We posit that this trend is likely driven by the fact that taxa with exposed anthers that experienced larger increases in temperature also experienced larger declines in ozone (r = −0.53, p = 0.001). Together, our results show that temporal change in floral pigmentation in species with concealed anthers was only influenced by temporal change in temperature whereas those with exposed anthers were more strongly affected by temporal change in ozone than temperature (Figure 4).

Table 3. The Magnitude of Climatic Change and Anther Exposure Determine Temporal Change in Floral Pigmentation

	Non-phylogenetic model		Phylogenetic Model	
Source	X^2	**P**	X^2	**P**
Floral shape	2.386	0.12	0.166	0.68
Life history	2.672	0.10	11.85	<0.001
Habitat	1.188	0.276	5.79	0.016
Temperature change	1.166	0.281	0.268	0.604
Ozone change	4.711	0.029	14.201	<0.001
Shape × temperature	6.99	0.008	6.296	0.012
Shape × ozone	4.16	0.041	5.00	0.025

Results from linear models predicting the response of pigmentation to time by floral shape (anthers exposed versus concealed), life history (short-lived versus perennial), habitat affinity (shaded versus open), the magnitude of temperature change, and the magnitude of ozone change. Results from a non-phylogenetically corrected model (GLM) and results from phylogenetic generalized least squares model (PGLS) accounting for a Brownian phylogenetic correlation structure are presented. Both models were tested with ANOVA using Type III sums of squares.

Whether the temporal change in floral pigmentation is explained by adaptation or phenotypic plasticity cannot be addressed from this study. Previous work shows a high degree of heritability for UV floral pigmentation [27, 28], but plastic responses of floral UV pigmentation patterns have yet to be shown [30]. However, UV-absorbing compounds (e.g., flavonoids) are often upregulated in response to elevated UV [18] and reduced temperatures [49], which are consistent with our findings. Visible petal coloration manifested by anthocyanin compounds which are produced in the same pathway as most UV-absorbing floral compounds, are frequently upregulated under cold stress as well (e.g., [47]). Thus, the potential for floral pigmentation plasticity in response to both ozone and temperature is strong. Differential plasticity among species in our study may thus account for some of the differential phenotypic responses over time, which is an area ripe for future work as it may impact plants' ability to respond to global change.

The effect of anthropogenic climatic change on floral pigmentation has implications for the future of plant-pollinator interactions and subsequent plant reproductive performance. As ozone degradation has been curbed since the enactment of the Montreal Protocol, minimal change in UV is expected on average across the globe. However, some regions are expected to experience large increases in UV under current emissions scenarios because of stratosphere-to-troposphere ozone flux [2]. Continued increases in pigmentation in response to increasing UV is therefore expected to display geographic heterogeneity. UV floral patterning caused by intrafloral contrast between UV-absorbing and -reflecting portions of petals increases attractiveness to pollinators relative to uniform floral UV absorption, in both wild [31] and crop species [34]. Thus, while elevated UV-absorbing pigmentation may afford higher pollen performance [17], pollinator-mediated pollen transfer could decline for some species if the loss of UV-reflection reduces overall floral attractiveness. While future changes in ozone will be geographically heterogenous, on average, temperature is expected to increase globally. Based on our data, we predict that the continuation of rising temperatures could lead to reduced UV pigmentation for species with concealed anthers. Thus, the trajectory of floral UV pigmentation is likely to reflect a balance of pressures to upregulate UV-absorbing compounds from elevated UV stress but pressure to downregulate them from rising temperatures.

STAR★METHODS

Detailed methods are provided in the online version of this paper and include the following:

- KEY RESOURCES TABLE
- RESOURCE AVAILABILITY
  - Lead Contact
  - Materials Availability
  - Data and Code Availability
- EXPERIMENTAL MODEL AND SUBJECT DETAILS
- METHOD DETAILS
  - Floral phenotyping
  - Geospatial and bioclimatic data
- QUANTIFICATION AND STATISTICAL ANALYSIS

SUPPLEMENTAL INFORMATION

Supplemental Information can be found online at https://doi.org/10.1016/j.cub.2020.08.077.

ACKNOWLEDGMENTS

We thank the staff at the following herbaria for access to collections: Botanische Staatssammlung München (M), Muséum national d'Histoire naturelle (P), National Herbarium of Victoria (MEL), The William & Lynda Steere Herbarium (NY), and Bonnie Isaac at Carnegie Museum's Herbarium (CM) for coordinating herbarium loans. We also thank Laura Galloway for access to lab space, and Amanda Murray, Momna Zainab, Parinita Kumar, Jeffery Gilman, Elizabeth O'Neill, and Gabriel Blanco for georeferencing specimens, photographing flowers, and analyzing images. This work was funded by NSF DEB 1753689 to T.-L.A. and NSF DEB 174590 to M.H.K.

AUTHOR CONTRIBUTIONS

M.H.K. and T.-L.A. designed the study, M.H.K. collected data, and M.H.K. and T.-L.A. managed processing of phenotypic and locality data. D.M. collected historical climatic data. M.H.K. analyzed the data and wrote the manuscript with input from T.-L.A. and D.M.

DECLARATION OF INTERESTS

The authors declare no competing interests.

Received: May 12, 2020
Revised: August 3, 2020
Accepted: August 24, 2020
Published: September 17, 2020

REFERENCES

1. Herman, J.R. (2010). Global increase in UV irradiance during the past 30 years (1979–2008) estimated from satellite data. J. Geophys. Res. *115*, D04203.
2. Hegglin, M.I., and Shepherd, T.G. (2009). Large climate-induced changes in ultraviolet index and stratosphere-to-troposphere ozone flux. Nat. Geosci. *2*, 687–691.
3. Williamson, C.E., Zepp, R.G., Lucas, R.M., Madronich, S., Austin, A.T., Ballaré, C.L., Norval, M., Sulzberger, B., Bais, A.F., McKenzie, R.L., et al. (2014). Solar ultraviolet radiation in a changing climate. Nat. Clim. Chang. *4*, 434–441.
4. Bornman, J.F., Barnes, P.W., Robinson, S.A., Ballaré, C.L., Flint, S.D., and Caldwell, M.M. (2015). Solar ultraviolet radiation and ozone depletion-driven climate change: effects on terrestrial ecosystems. Photochem. Photobiol. Sci. *14*, 88–107.
5. Roulin, A. (2014). Melanin-based colour polymorphism responding to climate change. Glob. Change Biol. *20*, 3344–3350.
6. Davis, M.B., Shaw, R.G., and Etterson, J.R. (2005). Evolutionary responses to changing climate. Ecology *86*, 1704–1714.
7. Aitken, S.N., Yeaman, S., Holliday, J.A., Wang, T., and Curtis-McLane, S. (2008). Adaptation, migration or extirpation: climate change outcomes for tree populations. Evol. Appl. *1*, 95–111.
8. Fitter, A.H., and Fitter, R.S. (2002). Rapid changes in flowering time in British plants. Science *296*, 1689–1691.
9. Crozier, L.G., and Hutchings, J.A. (2014). Plastic and evolutionary responses to climate change in fish. Evol. Appl. *7*, 68–87.
10. Davis, C.C., Willis, C.G., Connolly, B., Kelly, C., and Ellison, A.M. (2015). Herbarium records are reliable sources of phenological change driven by climate and provide novel insights into species' phenological cueing mechanisms. Am. J. Bot. *102*, 1599–1609.
11. Pang, Q., and Hays, J.B. (1991). UV-B-Inducible and Temperature-Sensitive Photoreactivation of Cyclobutane Pyrimidine Dimers in *Arabidopsis thaliana*. Plant Physiol. *95*, 536–543.
12. Jablonski, N.G., and Chaplin, G. (2010). Colloquium paper: human skin pigmentation as an adaptation to UV radiation. Proc. Natl. Acad. Sci. USA *107* (*Suppl 2*), 8962–8968.
13. Sinha, R.P., and Häder, D.-P. (2002). UV-induced DNA damage and repair: a review. Photochem. Photobiol. Sci. *1*, 225–236.
14. Rautio, M., and Korhola, A. (2002). UV-induced pigmentation in subarctic *Daphnia*. Limnol. Oceanogr. *47*, 295–299.
15. Bastide, H., Yassin, A., Johanning, E.J., and Pool, J.E. (2014). Pigmentation in *Drosophila melanogaster* reaches its maximum in Ethiopia and correlates most strongly with ultra-violet radiation in sub-Saharan Africa. BMC Evol. Biol. *14*, 179.
16. Santana, S.E., Lynch Alfaro, J., and Alfaro, M.E. (2012). Adaptive evolution of facial colour patterns in Neotropical primates. Proc. Biol. Sci. *279*, 2204–2211.
17. Koski, M.H., and Ashman, T.-L. (2015). Floral pigmentation patterns provide an example of Gloger's rule in plants. Nat. Plants *1*, 14007.
18. Barnes, P.W., Tobler, M.A., Keefover-Ring, K., Flint, S.D., Barkley, A.E., Ryel, R.J., and Lindroth, R.L. (2016). Rapid modulation of ultraviolet shielding in plants is influenced by solar ultraviolet radiation and linked to alterations in flavonoids. Plant Cell Environ. *39*, 222–230.
19. Agati, G., Brunetti, C., Di Ferdinando, M., Ferrini, F., Pollastri, S., and Tattini, M. (2013). Functional roles of flavonoids in photoprotection: new evidence, lessons from the past. Plant Physiol. Biochem. *72*, 35–45.
20. Searles, P.S., Flint, S.D., and Caldwell, M.M. (2001). A meta-analysis of plant field studies simulating stratospheric ozone depletion. Oecologia *127*, 1–10.
21. Ryan, K.G., Burne, A., and Seppelt, R.D. (2009). Historical ozone concentrations and flavonoid levels in herbarium specimens of the Antarctic moss *Bryum argenteum*. Glob. Change Biol. *15*, 1694–1702.
22. Thompson, W.R., Meinwald, J., Aneshansley, D., and Eisner, T. (1972). Flavonols: pigments responsible for ultraviolet absorption in nectar guide of flower. Science *177*, 528–530.
23. Harborne, J.B., and Nash, R.J. (1984). Flavonoid pigments responsible for ultraviolet patterning in petals of the genus *Potentilla*. Biochem. Syst. Ecol. *12*, 315–318.
24. Rieseberg, L.H., and Schilling, E.E. (1985). Floral Flavonoids and Ultraviolet Patterns in *Viguiera* (compositae). Am. J. Bot. *72*, 999–1004.
25. Gronquist, M., Bezzerides, A., Attygalle, A., Meinwald, J., Eisner, M., and Eisner, T. (2001). Attractive and defensive functions of the ultraviolet pigments of a flower (*Hypericum calycinum*). Proc. Natl. Acad. Sci. USA *98*, 13745–13750.
26. Sasaki, K., and Takahashi, T. (2002). A flavonoid from Brassica rapa flower as the UV-absorbing nectar guide. Phytochemistry *61*, 339–343.

27. Syafaruddin, Kobayashi, K., Yoshioka, Y., Horisaki, A., Niikura, S., and Ohsawa, R. (2006). Estimation of Heritability of the Nectar Guide of Flowers in *Brassica rapa* L. Breed. Sci. *56*, 75–79.

28. Koski, M.H., and Ashman, T.-L. (2013). Quantitative Variation, Heritability, and Trait Correlations for Ultraviolet Floral Traits in *Argentina anserina* (Rosaceae): Implications for Floral Evolution. Int. J. Plant Sci. *174*, 1109–1120.

29. Moyers, B.T., Owens, G.L., Baute, G.J., and Rieseberg, L.H. (2017). The genetic architecture of UV floral patterning in sunflower. Ann. Bot. *120*, 39–50.

30. Peach, K., Liu, J.W., and Mazer, S.J. (2020). Climate predicts UV floral pattern size, anthocyanin concentration, and pollen performance in *Clarkia unguiculata*. Front. Plant Sci. *11*, 847.

31. Koski, M.H., and Ashman, T.-L. (2014). Dissecting pollinator responses to a ubiquitous ultraviolet floral pattern in the wild. Funct. Ecol. *28*, 868–877.

32. Koski, M.H., and Ashman, T.-L. (2015). An altitudinal cline in UV floral pattern corresponds with a behavioral change of a generalist pollinator assemblage. Ecology *96*, 3343–3353.

33. Peterson, M.L., Miller, T.J., and Kay, K.M. (2015). An ultraviolet floral polymorphism associated with life history drives pollinator discrimination in *Mimulus guttatus*. Am. J. Bot. *102*, 396–406.

34. Brock, M.T., Lucas, L.K., Anderson, N.A., Rubin, M.J., Markelz, R.J., Covington, M.F., Devisetty, U.K., Chapple, C., Maloof, J.N., and Weinig, C. (2016). Genetic architecture, biochemical underpinnings and ecological impact of floral UV patterning. Mol. Ecol. *25*, 1122–1140.

35. Koski, M.H., and Ashman, T.-L. (2016). Macroevolutionary patterns of ultraviolet floral pigmentation explained by geography and associated bioclimatic factors. New Phytol. *211*, 708–718.

36. Zhang, C., Yang, Y.-P., and Duan, Y.-W. (2015). Pollen sensitivity to ultraviolet-B (UV-B) suggests floral structure evolution in alpine plants. Sci. Rep. *4*, 4520.

37. Savolainen, O., Bokma, F., García-Gil, R., Komulainen, P., and Repo, T. (2004). Genetic variation in cessation of growth and frost hardiness and consequences for adaptation of *Pinus sylvestris* to climatic changes. For. Ecol. Manage. *197*, 79–89.

38. Jump, A.S., and Penuelas, J. (2005). Running to stand still: adaptation and the response of plants to rapid climate change. Ecol. Lett. *8*, 1010–1020.

39. Borghi, M., Perez de Souza, L., Yoshida, T., and Fernie, A.R. (2019). Flowers and climate change: a metabolic perspective. New Phytol. *224*, 1425–1441.

40. van der Kooi, C.J., Kevan, P.G., and Koski, M.H. (2019). The thermal ecology of flowers. Ann. Bot. *124*, 343–353.

41. Meineke, E.K., Davis, C.C., and Davies, T.J. (2018). The unrealized potential of herbaria for global change biology. Ecol. Monogr. *88*, 505–525.

42. Johnson, A.L., Rebolleda-Gómez, M., and Ashman, T.-L. (2019). Pollen on stigmas of herbarium specimens: A window into the impacts of a century of environmental disturbance on pollen transfer. Am. Nat. *194*, 405–413.

43. Horovitz, A., and Cohen, Y. (1972). Ultraviolet reflectance characteristics in flowers of Crucifers. Am. J. Bot. *59*, 706–713.

44. Galeotti, P., Rubolini, D., Sacchi, R., and Fasola, M. (2009). Global changes and animal phenotypic responses: melanin-based plumage redness of scops owls increased with temperature and rainfall during the last century. Biol. Lett. *5*, 532–534.

45. Karell, P., Ahola, K., Karstinen, T., Valkama, J., and Brommer, J.E. (2011). Climate change drives microevolution in a wild bird. Nat. Commun. *2*, 208.

46. Sirkiä, P.M., Virolainen, M., Lehikoinen, E., and Laaksonen, T. (2013). Fluctuating selection and immigration as determinants of the phenotypic composition of a population. Oecologia *173*, 305–317.

47. Stiles, E.A., Cech, N.B., Dee, S.M., and Lacey, E.P. (2007). Temperature-sensitive anthocyanin production in flowers of *Plantago lanceolata*. Physiol. Plant. *129*, 756–765.

48. Djanaguiraman, M., Perumal, R., Jagadish, S.V.K., Ciampitti, I.A., Welti, R., and Prasad, P.V.V. (2018). Sensitivity of sorghum pollen and pistil to high-temperature stress. Plant Cell Environ. *41*, 1065–1082.

49. Rivero, R.M., Ruiz, J.M., García, P.C., López-Lefebre, L.R., Sánchez, E., and Romero, L. (2001). Resistance to cold and heat stress: accumulation of phenolic compounds in tomato and watermelon plants. Plant Sci. *160*, 315–321.

50. Schneider, C.A., Rasband, W.S., and Eliceiri, K.W. (2012). NIH Image to ImageJ: 25 years of image analysis. Nat. Methods *9*, 671–675.

51. R Core Team (2020). R: A language and environment for statistical computing (Vienna, Austria: R Foundation for Statistical Computing).

52. SAS Institute Inc. (2013). SAS version 9.4. (SAS Institute Inc.).

53. Hijmans, R.J., Cameron, S.E., Parra, J.L., Jones, P.G., and Jarvis, A. (2005). Very high resolution interpolated climate surfaces for global land areas. Int. J. Climatol. *25*, 1965–1978.

54. Caldwell, M., and Flint, S. (1994). Stratospheric ozone reduction, solar UV-B radiation and terrestrial ecosystems. Clim. Change *28*, 375–394.

55. Varotsos, C., Kondratyev, K.Ya., and Katsikis, S. (1995). On the relationship between total ozone and solar ultraviolet radiation at St. Petersburg, Russia. Geophys. Res. Lett. *22*, 3481–3484.

56. Webb, C.O., and Donoghue, M.J. (2005). Phylomatic: tree assembly for applied phylogenetics. Mol. Ecol. Notes *5*, 181–183.

57. Paradis, E., and Claude, J. (2002). Analysis of comparative data using generalized estimating equations. J. Theor. Biol. *218*, 175–185.

Please cite this article in press as: Koski et al., Floral Pigmentation Has Responded Rapidly to Global Change in Ozone and Temperature, Current Biology (2020), https://doi.org/10.1016/j.cub.2020.08.077

STAR★METHODS

KEY RESOURCES TABLE

REAGENT or RESOURCE	SOURCE	IDENTIFIER
Biological Samples		
1238 Herbarium Samples	Botanische Staatssammlung München; Muséum national d'Histoire naturelle; National Herbarium of Victoria; The William & Lynda Steere Herbarium	See Associated Data in Dryad Repository
Software and Algorithms		
ImageJ	[50]	https://imagej.nih.gov/ij/
R V. 3.6.3	[51]	https://www.r-project.org/
SAS v. 9.4	[52]	https://www.sas.com/en_us/home.html

RESOURCE AVAILABILITY

Lead Contact

Requests for any additional raw data and code should be directed to the lead contact, Matthew Koski (mkoski@clemson.edu).

Materials Availability

The dataset and the code ara avialble in DRYAD https://doi.org/10.5061/dryad.ttdz08kw1. Python scripts for acquisition of ozone and temperature data are available here: https://github.com/scholarslab/gis-ozone-temp-by-date-location.

Data and Code Availability

The dataset and code has been deposited in DRYAD, https://doi.org/10.5061/dryad.ttdz08kw1.

Python scripts for acquisition of ozone and temperature data are available here: https://github.com/scholarslab/gis-ozone-temp-by-date-location.

EXPERIMENTAL MODEL AND SUBJECT DETAILS

We selected 30 flowering plant species with exposed anthers (flowers radially symmetric or actinomorphic in shape), and 12 with concealed anthers (flowers bilaterally symmetric or zygomorphic in shape) representing 18 families and 22 genera (Figure S1; Table S1). Fourteen Australian, 19 Eurasian and 12 North American taxa were represented (n = 283, 643, 312 specimens respectively). Eurasian samples were collected from Botanische Staatssammlung München (M) and Muséum national d'Histoire naturelle (P); Australian samples from the National Herbarium of Victoria (MEL), and N. American samples from The William & Lynda Steere Herbarium (NY). We selected taxa based on the following criteria: first, they were known to possess UV patterning; second, they were well-represented in focal herbaria; third, 10 or more specimens had flowers pressed such that UV pigmentation could be scored non-destructively; fourth, the specimens spanned the time frame of interest (~1945-present). In total, we scored UV proportion unambiguously on 1238 specimens for an average of 27.5 specimens per taxon (range: 10-68). We originally selected 1630 specimens however the final dataset for analysis was smaller because some species were represented by fewer than 10 samples or UV pigmentation pattern was not reliably scored from images. The temporal range of specimens varied among taxa from 35 to 75 years. Three species with exposed anthers (*Caltha palustris, Argentina anserina, Cerastium arvense*) and one with concealed anthers (*Utricularia vulgaris*) were sampled from their distributions in both Eurasia and North America. We treated each continental distribution separately in analyses for these species because preliminary data showed that the same species responded differently to both time and climatic factors depending on their continental distribution.

METHOD DETAILS

Floral phenotyping

A single flower from each specimen was photographed with a UV-sensitive camera following [35].UV proportion ('UVP') was measured on a single petal as the area of UV absorption divided by the area of the petal in mm^2 using ImageJ [50] (see [28]). For two species, UVP was scored discretely. *Mimulus guttatus* specimens displayed UV patterning on the lower lobes of the flower (Figure 1). If the central and both lateral lobes were UV-absorbing, the pigmentation was scored as '1', if only the entire central lobe was UV-absorbing, it received a '0.5¢, and if the lower lobe was UV-reflecting it was scored as '0'. For *Utricularia vulgaris*, flowers were

Please cite this article in press as: Koski et al., Floral Pigmentation Has Responded Rapidly to Global Change in Ozone and Temperature, Current Biology (2020), https://doi.org/10.1016/j.cub.2020.08.077

pressed such that quantitative measurements of the UV absorbing area were difficult to conduct, however flowers either clearly displayed UV reflection, or were completely UV absorbing. These were scored as '0' for UV-reflecting and '1' for absorbing.

For each taxon we recorded life history and habitat affinity. Short-lived taxa included annuals and biennials while long-lived taxa included perennials. We obtained data on life history from online floras (e.g., Flora North America, Flora of Australia OnlineLife). Life history was included in analyses because the propensity to respond to global change may depend on generation time [37, 38]. Habitat type was either shaded (e.g., forest understory) or open (e.g., meadow species).

Geospatial and bioclimatic data

From each herbarium specimen, we recorded the date of collection (day, month, year), and the latitude and longitude if provided. The majority of specimens, however, lacked latitude and longitude data. Thus, we recorded detailed information on locality from herbarium annotations and used Google Maps and/or Google Earth to assign a latitude and longitude to each specimen to the best of our ability. Using these coordinates, we extracted altitude in meters from the Worldclim database using R [51, 53]. Latitude and longitude for the majority of specimens from Royal Botanic Garden Victoria were already georeferenced and linked with specimen barcodes. We used latitude and longitude coordinates to extract altitude (m) from the Worldclim dataset at a 2.5km grid scale using 'R'.

We obtained monthly average ozone (Dobson Units, DU) and monthly average temperature (°C) for the month of collection for each specimen. We used ozone instead of UV irradiance data because UV irradiance data are only available between 1979 and 2009. While UV irradiance can be modified by cloud cover and surface reflectivity, ozone is the primary predictor of UV-B irradiance [54, 55]. Specifically, ozone and UV irradiance are inversely related. Ozone data were downloaded from the WOUDC database (https://woudc.org) which curates ozone measurements from 525 globally-distributed weather stations. Tabular data on Monthly Average Ozone were joined to a layer of the monitoring station locations. This resulted in a point on the map for each year and month at each station. Using a custom Python script, we ran the Kriging tool to interpolate monthly-average ozone data for the month of collection for each specimen. An average of 111 stations (+/−1.59 SD) were used to interpolate ozone for each point.

Global Temperature anomalies CRUTEM4v and Absolute temperature NetCDF data were obtained from the Climate Research Unit website: https://crudata.uea.ac.uk/cru/data/temperature/. A custom Python script was used to sum the appropriate anomaly and absolute temperature rasters to obtain monthly average temperature for the date and location of collection for each specimen. All scripts are publicly available: https://github.com/scholarslab/gis-ozone-temp-by-date-location

Previous work has shown that within and among species, precipitation was not related to variation in UVP [17, 35]. Thus, we did not score historical precipitation for the current study.

QUANTIFICATION AND STATISTICAL ANALYSIS

To test whether UV pigmentation increased over time and if temporal change in pigmentation depended on floral shape (anthers exposed versus concealed), we modeled UVP as a function of year of collection and shape while accounting for taxonomic, geospatial and seasonal effects on pigmentation (spatiotemporal model). Specifically, we modeled UVP as a function of the following fixed effects: species identity nested within floral shape, floral shape, latitude, longitude, altitude, year of collection, and month of collection with continent (Australia, Europe, N. America) using a mixed general linear model in SAS (PROC MIXED [52],). Continent was used as a random effect in the model to account for regional differences in UVP (e.g., [17]). We included species identity to account for lineage-specific effects on pigmentation. Family could not be included because some families were represented by only one taxon (Table S1). We included latitude, altitude and longitude in the model because previous studies show broad regional, latitudinal and altitudinal effects on UVP [17, 32]. Finally, month was nested within continent was included in the model because bioclimatic factors expected to drive variation in pigmentation (temperature and ozone) display strong seasonal variation that differs across continents that span hemispheres. The model thus accounted for variance explained by taxonomic, geospatial, and seasonal parameters to test the independent effect of year on pigmentation. Finally, we tested for a species x year interaction with species nested within shape to determine whether there was species-specific pigmentation change over time. UVP was arcsine square-root transformed prior to analysis which improved normality, and model residuals were normally distributed. Using logit-transformed data, or raw data generated similar results.

To test the prediction that UVP would be negatively associated with ozone, we modeled UVP as a function of species nested within floral shape, floral shape, monthly temperature, monthly ozone, and the interaction between ozone and floral shape (climatic model). Continent was again used as a random term. Temperature was included first because it increased across the time span of our data collection and can be correlated with ozone (e.g., high latitudes have higher ozone than lower latitudes). Thus, inclusion of temperature in the model affords an evaluation of the independent effect of ozone. Second, temperature has been associated with variability in floral coloration in other systems [40] so may have a direct effect on UVP. Again, UVP was arcsine square-root transformed prior to analyses.

The spatiotemporal model revealed a strong species x year interaction (Table 1). To test whether species experiencing more drastic declines in ozone displayed more pronounced increases in pigmentation, we calculated the effect size of year on ozone, temperature, and UVP for each species. Specifically, for each species we modeled ozone, temperature and UVP separately as functions of latitude, longitude, altitude, and year using linear models. These models estimated the effect of the year of specimen collection on UVP, temperature, and ozone for each species while accounting for geospatial variation. We standardized all variables in the model to extract the standardized effect of year on each parameter. Standardized slopes of ozone, temperature and UVP on year are hereafter

Please cite this article in press as: Koski et al., Floral Pigmentation Has Responded Rapidly to Global Change in Ozone and Temperature, Current Biology (2020), https://doi.org/10.1016/j.cub.2020.08.077

considered 'ozone change', 'temperature change' and 'UVP change', respectively, as they are a metric of change over time. We modeled UVP change as a function of floral shape, ozone change, temperature change, habitat affinity (open versus shaded), and life history (perennial versus short-lived) using a linear model. The model was weighted by the number of samples for each species. Habitat type may impact response to ozone decline because understory species are likely to be more protected from UV. We tested for two-way interaction terms between floral shape and climatic variables (ozone change, temperature change). Initial analyses included two-way interaction between life history and climatic variables, and habitat type and climatic variable that were non-significant and removed from the final model.

To test whether results were robust to the inclusion of variance explained by phylogenetic relatedness, we generated a phylogeny of all species using Phylomatic [56] (Figure S1). For species that were represented on multiple continents, we added tips to the phylogeny whereby the same taxa on different continents were considered sisters. We set branch lengths equal to 1 using the 'brlen' function [57]. We constructed a PGLS model using the 'gls' function and a the phylogeny with a Brownian Motion correlation structure. We again modeled the change in UVP as a function of shape, ozone change, temperature change, life history and the interaction between shape and ozone change, and shape and temperature change.

Current Biology, Volume *30*

Supplemental Information

Floral Pigmentation Has Responded Rapidly to Global Change in Ozone and Temperature

Matthew H. Koski, Drew MacQueen, and Tia-Lynn Ashman

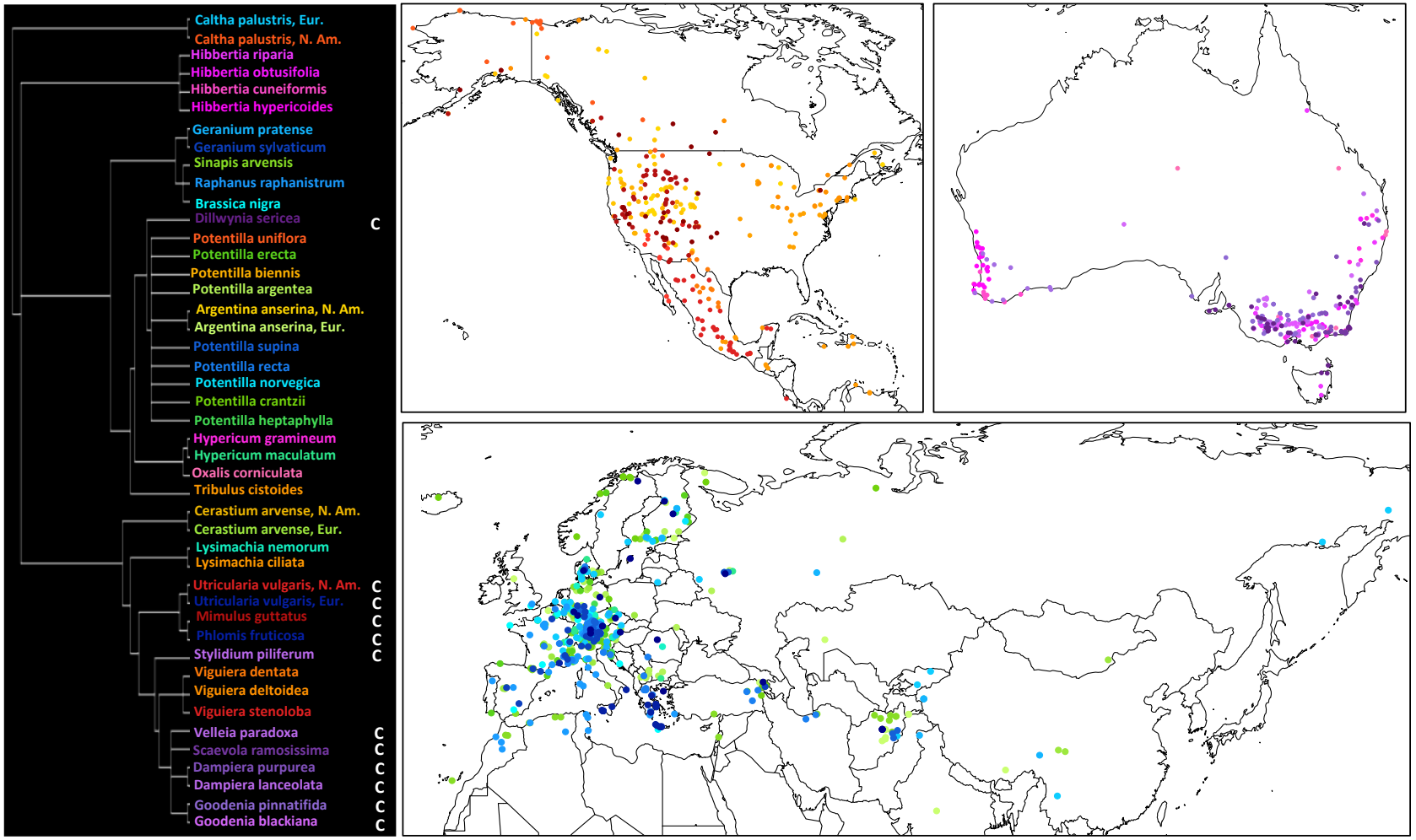

Figure S1: Phylogenetic and geographic distribution of specimens. Related to "Experimental model and subject details" in STAR Methods. For all specimens, UV floral pigmentation was associated with date of collection, and ozone and temperature at the time of collection. North American taxa are plotted in gold to red, Australian in pink to purple, and Eurasian in green to blue. Each point on the maps represents a single herbarium specimen (N=1238). Taxa with anthers concealed within floral tissue are denoted by a 'C' on the phylogeny. All other taxa have flowers with anthers exposed.

Continent	Family	Genus	Species	Floral Shape	Life History	Habitat	Samples	Standardized slope of UVP on year	Standardized slope of ozone on year	Standardized slope of temperature on year	First Year	Last Year	Year Range
Australia	Dilleniaceae	Hibbertia	cuneiformis	E	p	o	11	-0.341	0.280	0.209	1947	1993	46
Australia	Dilleniaceae	Hibbertia	hypericoides	E	p	o	22	-0.014	-0.059	0.485	1963	2004	41
Australia	Dilleniaceae	Hibbertia	obtusifolia	E	p	o	18	-0.251	-0.156	-0.002	1964	2016	52
Australia	Dilleniaceae	Hibbertia	riparia	E	p	o	25	-0.018	0.150	0.034	1966	2017	51
Australia	Fabaceae	Dillwynia	sericea	C	p	o	39	-0.172	0.085	0.196	1946	2015	69
Australia	Goodeniaceae	Dampiera	purpurea	C	p	o	14	0.236	0.000	0.129	1958	2005	47
Australia	Goodeniaceae	Goodenia	blackiana	C	p	o	39	-0.142	0.159	0.168	1947	2015	68
Australia	Goodeniaceae	Goodenia	pinnatifida	C	p	o	32	-0.105	-0.285	0.165	1950	2017	67
Australia	Goodeniaceae	Scaevola	ramosissima	C	p	o	11	0.282	-0.071	-0.213	1953	2004	51
Australia	Goodeniaceae	Velleia	paradoxa	C	p	o	20	0.616	-0.041	-0.044	1960	2013	53
Australia	Goodeniaceae	Dampiera	lanceolata	C	p	o	11	-0.341	0.005	0.403	1969	2012	43
Australia	Hypericaceae	Hypericum	gramineum	E	p	o	19	0.197	-0.024	0.020	1960	2015	55
Australia	Oxalidaceae	Oxalis	corniculata	E	p	o	12	-0.122	0.109	-0.124	1957	2010	53
Australia	Stylidiaceae	Stylidium	piliferum	C	p	o	10	-0.007	0.798	0.604	1946	1995	49
Eurasia	Brassicaceae	Brassica	nigra	E	s	o	17	0.363	-0.410	0.076	1952	2001	49
Eurasia	Brassicaceae	Raphanus	raphanistrum	E	s	o	44	-0.083	-0.260	0.335	1950	2015	65
Eurasia	Brassicaceae	Sinapis	arvensis	E	s	o	39	0.094	-0.465	0.244	1950	2016	66
Eurasia	Caryophyllaceae	Cerastium	arvense	E	p	o	22	0.644	-0.143	0.140	1949	2011	62
Eurasia	Geraniaceae	Geranium	pratense	E	p	o	28	0.155	0.333	-0.307	1952	2009	57
Eurasia	Geraniaceae	Geranium	sylvaticum	E	p	s	29	-0.180	-0.111	-0.225	1947	2004	57
Eurasia	Hypericaceae	Hypericum	maculatum	E	p	o	24	-0.291	-0.040	-0.240	1959	2012	53
Eurasia	Lamiaceae	Phlomis	fruticosa	C	p	o	23	0.401	-0.206	-0.363	1952	2015	63
Eurasia	Lentibulariaceae	Utricularia	vulgaris	C	p	o	21	0.118	-0.075	0.115	1949	2013	64
Eurasia	Primulaceae	Lysimachia	nemorum	E	p	s	19	-0.276	0.081	-0.088	1946	1998	52
Eurasia	Ranunculaceae	Caltha	palustris	E	p	s	60	-0.175	-0.263	0.336	1943	2014	71
Eurasia	Rosaceae	Potentilla	anserina	E	p	o	41	-0.022	0.117	0.020	1947	2017	70
Eurasia	Rosaceae	Potentilla	argentea	E	p	o	68	-0.015	-0.212	0.159	1950	2015	65
Eurasia	Rosaceae	Potentilla	crantzii	E	p	o	58	-0.013	0.089	-0.140	1948	2014	66
Eurasia	Rosaceae	Potentilla	erecta	E	p	o	62	-0.245	0.019	0.009	1950	2016	66
Eurasia	Rosaceae	Potentilla	heptaphylla	E	p	o	28	0.054	-0.482	0.009	1950	2017	67
Eurasia	Rosaceae	Potentilla	norvegica	E	s	o	12	0.202	-0.721	0.343	1948	2013	65
Eurasia	Rosaceae	Potentilla	recta	E	p	o	37	-0.309	0.095	-0.124	1946	2010	64
Eurasia	Rosaceae	Potentilla	supina	E	s	o	11	0.032	-0.496	0.481	1957	2006	49
N. America	Asteraceae	Viguiera	deltoidea	E	p	o	10	0.912	-0.777	0.360	1952	1992	40
N. America	Asteraceae	Viguiera	dentata	E	p	o	36	0.335	-0.020	0.159	1953	2007	54
N. America	Asteraceae	Viguiera	stenoloba	E	p	o	13	0.071	-0.004	0.523	1962	1997	35
N. America	Caryophyllaceae	Cerastium	arvense	E	p	o	27	0.045	0.121	-0.348	1953	2007	54
N. America	Lentibulariaceae	Utricularia	vulgaris	C	p	o	24	0.309	0.314	-0.228	1950	2000	50
N. America	Phyrmaceae	Mimulus	guttatus	C	s	o	56	-0.078	0.108	-0.078	1952	2013	61
N. America	Primulaceae	Lysimachia	ciliata	E	p	s	26	0.213	-0.309	0.032	1950	2013	63

N. America	Ranunculaceae	Caltha	palustris	E	p	s	25	-0.246	0.025	0.011	1948	2014	66
N. America	Rosaceae	Potentilla	anserina	E	p	o	42	-0.184	-0.230	0.068	1941	2009	68
N. America	Rosaceae	Potentilla	biennis	E	s	o	18	-0.491	0.161	-0.410	1950	2008	58
N. America	Rosaceae	Potentilla	uniflora	E	p	o	16	0.558	0.240	0.062	1953	2001	48
N. America	Zygophyllaceae	Tribulus	cistoides	E	p	o	19	0.328	-0.059	0.207	1954	1993	39

Table S1: **Taxa included in study testing for temporal, spatial and climatic effects on floral UV pigmentation**. **Related to "Experimental model and subject details" in STAR Methods.** Continental distribution, family, genus, species, floral shape (E=anthers exposed, C=anthers concealed), life history (p=perennial, s=short-lived), habitat type (o=open, exposed; s= shaded), the number of samples per taxon, and the temporal distribution of samples are provided. Additionally, the standardized slope of UVP, ozone, and temperature across the years sampled are provided.